The immune microenvironment in patients with mismatch-repair-proficient oligometastatic colorectal cancer exposed to chemotherapy: the randomized MIROX GERCOR cohort study

Marine Jary, Wen-wei Liu, Dongyao Yan, Isaac Bai, Andrea Muranyi, Elise Colle, Isabelle Brocheriou, Anthony Turpin, Nina Radosevic-robin, Pierre Bourgoin, et al.

DR. MARINE JARY (Orcid ID : 0000-0001-7502-7708)

Received Date : 17-May-2021
Revised Date : 26-Nov-2021
Accepted Date : 23-Dec-2021
Article type : Research Article

The immune microenvironment in patients with mismatch-repair-proficient oligometastatic colorectal cancer exposed to chemotherapy: the randomized MIROX GERCOR cohort study

Marine Jary[1-2], Wen-Wei Liu[3], Dongyao Yan[3], Isaac Bai[3], Andrea Muranyi[3], Elise Colle[4], Isabelle Brocheriou[5], Anthony Turpin[1,6], Nina Radosevic-Robin [7], Pierre Bourgoin[8], Frédérique Penault-Llorca[7], Romain Cohen[1,9], Dewi Vernerey[1,10,11], Thierry André[1,9], Christophe Borg[1,11,12], Kandavel Shanmugam[3 #], Magali Svrcek[1,8 #]

#: *KS and MS contributed equally to this work*

1. Multidisciplinary Group in Oncology (GERCOR), Paris, France
2. Department of Surgical and Medical Oncology, University Hospital of Clermont-Ferrand, Clermont-Ferrand, France
3. Ventana Medical Systems Inc., Tucson, Arizona, USA
4. Department of Medical Oncology, University Hospital of Beaujon, Clichy, France
5. Sorbonne University, Department of Pathology, Assistance Publique-Hôpitaux de Paris, Pitié-Salpêtrière Hospital, Paris, France

6. Department of Medical Oncology, University Hospital of Lille, Lille, France
7. IMoST - Molecular Imaging & Theranostic Strategies, Clermont-Ferrand, France
8. Sorbonne University, Department of Pathology, Assistance Publique-Hôpitaux de Paris, Saint-Antoine Hospital, Paris, France
9. Sorbonne University, Department of Medical Oncology, Assistance Publique-Hôpitaux de Paris, Saint-Antoine Hospital, Paris, France
10. Methodology and Quality of Life in Oncology Unit, Besançon University Hospital, Besançon, France
11. INSERM, EFS BFC, UMR1098, RIGHT, University of Bourgogne Franche-Comté, Interactions hôte-greffon-tumeur/Ingénierie Cellulaire et Génique, Besançon, France
12. Department of Medical Oncology, University Hospital of Besançon, Besançon, France

Running title: Immune profile of pMMR omCRC

Keywords:
Oligometastatic colorectal cancer, pMMR, immune profile, T lymphocytes, PD-L1

Correspondence to:
Dr Kandavel Shanmugam, Medical Innovation, Clinical Science, Roche Tissue Diagnostics, Tucson, AZ, USA; Email: kandavel.shanmugam@roche.com
Pr Magali SVRCEK, Sorbonne Université, Assistance Publique-Hôpitaux de Paris, Department of Pathology, Saint-Antoine Hospital, Paris, France; Tel: +33(0)149282179, Fax: +33(0)149282878, Email: magali.svrcek@aphp.fr

ABBREVIATIONS

CC1 buffer: Cell Conditioning 1 buffer
CEA: CarcinoEmbryonic Antigen
CI: Confidence Interval
CMS: Consensus Molecular Subtype
CRC: Colorectal cancer
DFS: Disease-free survival
dMMR/MSI: deficient mismatch repair /microsatellite instable
FFPE: Formalin-fixed, paraffin-embedded
FOXP3: Forkhead box protein 3
GERCOR: Groupe Coopérateur Multidisciplinaire en Oncologie
HR: Hazard ratios
ICIs: Immune checkpoint inhibitors
IE: intra-epithelial
IF: invasive front
IFN-γ: Interferon Gamma
IHC: Immunohistochemistry
mCRC: metastatic CRC
MDSC: Myeloid derived suppressor cell
MEK: Mitogen-activated protein kinase kinase
MHC: Major histocompatibility complex
MLH1: MutL homolog 1
MSH2: MutS homolog 2
MSH6: MutS homolog 6
omCRC: oligometastatic CRC
PD-1: Programmed cell death protein 1
PD-L1: Programmed death ligand 1
pMMR/MSS: proficient mismatch repair/microsatellite stable
PMS2: PMS1 homolog 2
TILs: Tumor-infiltrating lymphocytes
TRG: Tumor regression grade

Molecular Oncology (2020) © 2020 The Authors. Published by FEBS Press and John Wiley & Sons Ltd.

ABSTRACT

In the era of immune checkpoint inhibitors, understanding the metastatic microenvironment of proficient mismatch repair/microsatellite stable (pMMR/MSS) colorectal cancer (CRC) is of paramount importance to both prognostication and the development of more effective novel therapies. In this study, primary and paired metastasis tissue samples were collected from patients with resectable metastatic CRC treated with adjuvant FOLFOX or peri-operative chemotherapy in the MIROX phase III prospective study. In total, 74 cancer tissues were stained for CD3, CD8, Forkhead box protein 3 (FOXP3), Programmed cell Death protein-1(PD-1, invasive front, stromal, intra-epithelial compartments) and Programmed Death-Ligand 1 (PD-L1, tumor, immune cells). The immune profiling of primary CRC had a limited value to predict the immune context of paired metastases for all markers but CD3+. The expression of CD8 and PD-L1 was higher in metastases after neoadjuvant FOLFOX. In metastases, both CD3 T cells at the invasive front and PD-L1 expressions on immune cells were predictive of better disease-free survival. These results show that the effect of FOLFOX on modifying the immune microenvironment in resected CRC metastases and measurement of PD-L1 expression and tumor-infiltrating CD8 T cells in pMMR/MSS metastatic tissue samples could improve treatment strategies of metastatic CRC patients.

1. Introduction

Accumulating evidence suggests that the adaptive immune system can influence cancer progression and that the quantification of tumor-infiltrating lymphocytes (TILs) may improve prognostic ability of the staging system in patients with solid tumors. In colorectal cancer (CRC), the impact of immune cell infiltration in the primary tumor on survival has been demonstrated [1,2]. Patients with metastatic CRC (mCRC) in the liver have heterogeneous clinical outcomes. Indeed, 70% of patients with curatively resected metastases will relapse and half of these will ultimately die [3,4]. Clinico-pathological prognostic factors like the tumor regression grade (TRG) have been proposed to identify patients who may be at risk for recurrence [5], but none of these markers has been sufficiently informative to correctly predict the outcome. In the era of personalized medicine, an identification of prognostic and predictive biomarkers is essential. Regarding mCRC, the immune microenvironment of the liver metastases reflects an important aspect of the overall portrait of the patient's disease, especially the heterogeneity compared to the primary tumor and its clinical impact [6–9]. The immune microenvironment of colorectal metastases has not been fully investigated, and published studies are often limited to CD4, CD8, and regulatory T cells [10]. In addition, several chemotherapy regimens such as oxaliplatin seem to have a preponderant role in anti-tumor immunologic infiltration, with a stimulating effect on the peritumoral immune response [11,12]. In particular, immunogenic cell death is provoked by FOLFOX and accompanied by tumor-targeting immune responses, release of damage-associated molecular patterns, and recruitment of antigen-presenting immune cells. Interestingly, the EORTC phase III study 40983 of 82 patients with resected colorectal liver metastases (38 in the surgery with perioperative FOLFOX chemotherapy arm and 44 in the surgery alone arm) [13] showed for the first time that chemotherapy influences immune cell profiles, independent of patient characteristics. In this latter study, abundance of CD3 T cell lymphocytes at the invasive margin of the resected metastasis specimens appeared to be prognostic. Moreover, immune infiltration of lymphocytes was associated with increased progression-free survival.

The efficacy of immune checkpoint inhibitors (ICIs) in mismatch repair deficient (dMMR)/microsatellite instable (MSI) mCRC is now well established [14–18]. However, questions remain regarding the role of ICIs for the treatment of MMR-proficient (pMMR)/microsatellite stable (MSS) mCRC. The combination of ICIs with other anticancer drugs is currently being evaluated in pMMR/MSS mCRC. The disappointing results of the phase III IMblaze 370 trial (atezolizumab with or without cobimetinib *versus* regorafenib) raise concerns

regarding the testing ICI-based strategies without decision-guiding biomarkers in pMMR/MSS mCRC. Contrarily, the NICHE study provided hypothesis-generating data for patients with localized pMMR/MSS colon cancer [19]. Thus, deeper understanding of the metastatic microenvironment of pMMR/MSS mCRC, and particularly oligometastatic CRC (omCRC) could improve selection of patients who may benefit from ICI combinations and other immunogenic drugs such as oxaliplatin.

Programmed Death-Ligand 1 (PD-L1) is expressed by tumor cells and certain immune cell types (dendritic cells, macrophages, B lymphocytes, Natural Killer cells). T-cells expressing Programmed cell Death protein-1 (PD-1) exhibit suppressed proliferation through PD-1/PD-L1 interaction. However, PD-1 and PD-L1 expression in primary CRC are associated with favorable outcomes [20,21]. In most cancers treated with anti-PD-1 or anti-PD-L1 antibodies, the response rate is often higher in tumors expressing higher levels of PD-L1-positive immune cells. PD-L1-expressing tumor cells have been shown to regulate host immunity in the CRC microenvironment [22]. In the pMMR cohort of the NICHE study, the presence of T cells with co-expression of CD8 and PD-1 was the only biomarker found to predict major or partial pathological response [19]. Data regarding the expression of PD-L1 in CRC liver metastases and notably the interactions of PD-L1 with elements of the immune tumor microenvironment, as well as patient outcome, have recently been described [23]. No correlation between tumor-specific PD-L1 expression and survival was shown, confirming the results from other studies [24]. However, contradictory results are observed between the metastatic and early-stage settings [25], and few study yet assessed the expression of PD-L1 in a homogeneous cohort of matched primary and metastatic pMMR/MSS omCRC [26].

In this study we aimed to extensively characterize the immune microenvironment in patients with resectable mCRC treated or not with neoadjuvant FOLFOX to highlight an immunologic signature in this setting. We described potential tumor heterogeneity in chemo-naive patients with synchronous metastases and investigated if the immune infiltrate in resected colorectal metastases could be predictive of survival. The influence of FOLFOX-based chemotherapy and PD-1 and PD- L1 expression on the immune microenvironment and patient survival was further investigated.

2. MATERIALS AND METHODS

2.1. Study population

In total, 74 mCRC patients with available tissues from both primary tumors and paired metastases out of 284 included in the open-label prospective phase III MIROX trial were analyzed in this analysis. Patients with resectable or resected synchronous or metachronous metastases (only one site in liver, lung, ovary, or peritoneum) were treated with 6 cycles of FOLFOX4 (oxaliplatin 85 mg/m^2) or FOLFOX7 (oxaliplatin 130 mg/m^2) before metastasis resection followed by adjuvant chemotherapy (FOLFOX or FOLFIRI). The dose of oxaliplatin was randomly assigned at the beginning of the study [27]. The primary CRC was resected before diagnosis of metastasis and neoadjuvant chemotherapy. This trial was approved by the local Ethics Committees at participating GERCOR (*Groupe Coopérateur Multidisciplinaire en Oncologie*) centers. All patients provided their written informed consent to receive treatment and participate in translational analysis.

Formalin-fixed, paraffin-embedded (FFPE) primary CRC tumor specimens were obtained prior to chemotherapy. Paired metastatic lesions were collected prior to adjuvant chemotherapy or after neoadjuvant chemotherapy and centralized at the Department of Pathology, Saint-Antoine Hospital (Paris, France), constituting the study cohort, BIOMIROX. Pathological response of CRC liver metastasis in patients treated with perioperative chemotherapy was estimated by the TRG pathological response score [5]. The study methodologies conformed to the standards set by the Declaration of Helsinki.

2.2. Immunohistochemistry analysis

Immunohistochemistry (IHC) staining was performed on serial sections from surgically resected specimens (VENTANA BenchMark ULTRA automated staining instrument at Pitié-Salpêtrière Hospital). Briefly, FFPE tissue sections were deparaffinized, pretreated with Cell Conditioning 1 for antigen retrieval, and treated to inactivate the endogenous peroxidase and then incubated with CONFIRM anti-CD3 (2GV6) rabbit monoclonal antibody, anti-CD8 (SP239) rabbit monoclonal antibody, anti-FOXP3 (SP97) rabbit monoclonal antibody, anti-PD-1 (NAT105) mouse monoclonal antibody, and anti-PD-L1 (SP263) rabbit monoclonal antibody. Staining was visualized using the OptiView DAB IHC Detection Kit (Ventana Medical System, Inc.). Following detection, all slides were counterstained with hematoxylin II and bluing reagent for 4 minutes each, and coverslips were applied.

The density of tumor infiltrating immune CD3 and CD8 T cells was semi-quantitatively scored at the invasive front (IF; cells localized in stroma adjacent to the invasive tumor margin) and the intra-tumoral (or stromal) compartment [28] and graded as follows: 0, no positive cells; 1, scattered positive cells; 2, moderate number of positive cells; 3, abundant occurrence of positive cells. For CD3 T cells, the intra-epithelial (IE) compartment was also assessed. PD-1 and FOXP3 were scored semi-quantitatively, both at the IF and stromal compartment, as follows: 0, no positive cell or scattered cells; 1, moderate number of positive cells, and 2, numerous positive cells. Positive PD-L1 expression was defined as any staining ≥1%, in either infiltrating inflammatory cells or membranous-site tumor cells [29]. The percentage of cells demonstrating PD-L1 staining was scored in 5% increments and high PD-L1 level was defined as ≥5%, based on published literature [30-34]. Tissue samples were evaluated by an experienced pathologist (MS) blinded to clinical information, treatment regimens, and outcomes (**Table S1**).

Tumor tissue sections were double-stained for PD-L1 and CD8 using a fully automated procedure in a Benchmark Ultra automate (Ventana/Roche). Epitope retrieval was performed in Cell Conditioning 1 (CC1 buffer) for 60 min at 95°C. PD-L1 was detected by Ventana PD-L1 SP263 Assay (Roche Diagnostics, Meylan, France), per manufacturer's instructions. CD8 was detected by clone SP239 (Abcam, Cambridge, UK) at 1/100 for 60 min at room temperature. For PD-L1, the antigen-antibody reaction was revealed by OptiView DAB IHC Detection Kit, and for CD8 by UltraView Universal AP Red Detection Kit (red signal), both from Roche Diagnostics (Meylan, France). Co-staining was appreciated by a semi-quantitative method.

The expression of MutL homolog 1 (MLH1, dilution 1/70, clone G168-728, Pharmingen, San Diego, CA), MutS homolog 2 (MSH2, dilution 1/100, clone FE11, Calbiochem, Oncogene Research Products, Cambridge, MA), MutS homolog 6 (MSH6, dilution 1/100, clone 44, Becton Dickinson, Lexington, NC), and PMS1 homolog 2 (PMS2 , clone A16-4, 1:150 dilution, BD PharMingen, Le Pont de Claix, France) was assessed. Immunostaining of MLH1, MSH2, MSH6, and PMS2 in tumor cells was evaluated as positive (mismatch repair [MMR]-proficient [pMMR]) or negative (MMR-deficient [dMMR]). Tumors were considered negative when there was a complete absence of nuclear staining of neoplastic cells in the presence of an internal positive control.

2.3. **Statistical analysis**

All IHC markers but PD-L1 were semi-quantitatively assessed. Therefore, they were treated as categorical variables in this study. The Cox proportional-hazards model was used to estimate hazard ratios (HRs) and *P* values with disease-free survival (DFS). The association between clinical, biomarker parameters, and survival was estimated with univariate Cox proportional hazards models and HR with 95% Confidence Interval (CI) were given. Multivariate Cox models were investigated including clinico-biological parameters with p value <0.05 in univariate analysis. P value <0.05 was considered statistically significant. Spearman correlations between metastatic immune infiltrate and TRG scoring were estimated. Analyses were performed by SAS version 9.4 (SAS Institute Inc, Cary, NC).

3. RESULTS

3.1. Study cohort characteristics

A total of 74 patients with pMMR CRC were included in the current study. All baseline characteristics are summarized in **Table S2** and in the flowchart (**Fig. S1**). The median age of patients was 61 years (range 29-75). Forty-one patients had nearby lymph node metastases of the primary, and 82.6% were left-sided tumors (including rectum). Most patients (*n* = 65) had liver-only metastases and nine had another only one site of distant metastases (lung [*n* = 3], ovary [*n* = 1], peritoneal location [*n* = 5]). The median number of metastases was 2 (range, 1-7). Twenty-four patients had metachronous metastases. The mean preoperative CarcinoEmbryonic Antigen (CEA) level was 55.9 ng/mL (*n* = 70). Out of the 74 patients analyzed, 34 received adjuvant chemotherapy after surgery of their metastases ("chemo-naïve" patients). Among patients treated with neoadjuvant chemotherapy, two did not receive oxaliplatin.

3.2. Immune profiling between the primary CRC and matched metastasis

The distribution of semi-quantitative scores of CD3, CD8, FOXP3, PD-1, and PD-L1 (**Fig. 1, Table 1, Table S1, Fig.S2**) showed considerable heterogeneity, both in primary tumors and metastases, in chemo-naïve patients and those treated with neoadjuvant chemotherapy before surgery. Infiltration of CD3 T lymphocytes was the strongest in stroma and the IF both in primary tumors and metastases.

To avoid the potential confounding effect of chemotherapy on immune cell infiltration, we further examined the distribution scores by restricting the analyses to 34 chemo-naïve patients only (**Fig. S2**). The vast majority of these patients (n = 31) demonstrated high density of CD3 T cells (IHC score 2-3) in the IF of metastatic sites (liver [n = 25], lung [n = 2], ovary [n = 1], peritoneal [n = 3]). Seventeen patients in the chemo-naïve cohort had a high expression of CD3 cells (IHC 2 and 3) in the IF of the primary tumor (**Table 1**). Interestingly, this expression was strongly correlated (16 out of 17 patients, 94%) with that observed in the metastases compared but it was not the case for stromal and intraepithelial compartments CD3 cells (IHC 2 and 3) of the primary tumor and their matched metastases (**Table 1 and Table S1**).

PD-1 overexpression on CD8 T cells is known as an exhaustion biomarker, but it also reflects antigen-experienced lymphocytes. Conversely, PD-L1 expression on tumor or immune cells is induced by an interferon-mediated signaling. We characterized therefore CD3 and CD8 expression according to PD-L1 expression in the pMMR/MSS mCRC study cohort. A high level of PD-L1 expression was observed predominantly in immune cells (20 [58.8%] vs 3 [8.8%] in tumoral cells; **Table S1**) in CRC. Among the 33 patients for whom CD8 staining was available, four had high CD8 immune infiltrate (IHC score 2-3) in the IF of the primary tumor (**Table S1**). Three of the latter patients had a PD-L1 expression >5% in immune cells ($CD8^{high}$/$PD\text{-}L1^{high}$ patients; **Fig. 1).** Of the 29 patients with low CD8 score, 17 showed high PD-L1 expression ($CD8^{low}$/$PD\text{-}L1^{high}$ patients; **Table 1 and Table S1**). By comparison, twenty-six patients had low CD8 immune infiltrate in the IF of metastases, 10 of whom were classified as $PD\text{-}L1^{low}$ (<5%; $CD8^{low}$/$PD\text{-}L1^{low}$). Seven patients had high CD8 T cell infiltration in the IF. In all these patients, a high PD-L1 score (≥5% of expression by immune cells; **Fig. 1, Table 1, and Table S1**) was observed. In order to better appreciate the co-localization of CD8 and PD-L1, their co-staining was performed in six of these seven patients. The co-localization of CD8 and PD-L1 was observed in ≥20% of inflammatory cells. In four out of seven cases, a co-localization was detected in over 50% of cells. Negative controls had no more than 10% of co-localization detected (**Fig. S3**).

Regulatory T cells in CRC have been described in the non-inflamed tumors because of their tolerance properties, but they also play a role for effector T cells, which is to maintain immune homeostasis, even when the anti-tumor immune response is active [35-37]. In our study, half of the $CD8^{high}$/$PD\text{-}L1^{high}$ patients had high immune IF FOXP3 infiltration.

Contrary to CD3 staining, the analysis showed that CD8 and PD-L1 expressions were slightly less correlated between the primary tumors and matched metastases. Fifteen of the 20

patients with a high PD-L1 expression (i.e. at least 5% of positive immune or tumoral cells) in the primary tumor had also high PD-L1 expression in the matched metastasis (**Table 1 and Table S1**). Three out of four patients with high CD8 expression in the primary tumor had also more CD8 T-cell infiltration in their metastasis. Three patients showing positive PD-L1 staining in the primary tumor were negative/low for PD-L1 in the matched metastasis but showed a high CD3 immune infiltration (IHC score 2-3) in the IF of the metastatic tumor.

The above data suggested that the immune profiling performed on the primary tumor has a limited predictive value to estimate the immune context of metastasis. Further analysis focused on the tumor-infiltrating immune cell in metastasis.

3.3. **Patients' characteristics according to the expression of IF CD3, IF CD8, and immune PD-L1 in metastases of chemo-naive patients**

The clinical characteristics of 34 chemo-naive patients according to the expression of IF CD3, IF CD8, and immune cells PD-L1 in metastatic tumors are described in **Table 2**. Most of patients with high IF CD3 expression in metastatic tumors (out of 31 [96.7%]; IHC score 2+ and 3+) and all patients with and CD8+ and PD-L1 in metastases (n = 7) had tumors less than 5 cm in diameter and 70% (21 out of 31 patients) and 85%, respectively, had only one metastatic site. The CEA level before metastases resection was low in these patients.

3.4. **Patient and biomarker characteristics according to neoadjuvant chemotherapy: the impact of neoadjuvant FOLFOX on immune infiltrate in metastases**

Oxaliplatin-based chemotherapy can release antigens and promote immunogenic cell death leading to a specific anti-tumor immune response. Therefore, we further examined the distribution and type of the immune cell infiltration in patients with or without neoadjuvant FOLFOX chemotherapy (**Table 1, Table S3**). Patients with chemotherapy-treated metastatic sites had metastases strongly (IHC 3) positive for CD3 cells at IF (28.2% versus 14.7%), moderately (IHC 2)/strongly positive for CD3 cells in stroma (47.5% versus 32.4%), and moderately/strongly positive for CD8 cells at IF (41.1% versus 21.2%) than patients whose metastases were not exposed to chemotherapy. FOXP3 reg T cell staining was relatively weak but significantly decreased in the IF after chemotherapy (P = 0.0010). Of interest, seven chemo-naive patients (out

of 33; 21%) had high CD8 and high /PD-L1 staining versus 13 who received FOLFOX-based chemotherapy (out of 38; 34%).

These results suggested that chemotherapy may impact the immune microenvironment of patients and increase CD8 and PD-L1 expression in metastases.

Finally, a significant inverse correlation between $CD3^{high}$ T cell infiltration in stroma and TRG was observed, reflecting a better pathological response in CD3 T cells-inflamed tumors (Spearman correlation -0.33, $P = 0.0484$; **Table S4**).

3.5. **Association between the immune infiltrate and survival in metastases**

In the univariate analysis, low IF CD3 in metastases correlated with a shorter DFS (**Table 3**). Patients with a higher number of metastases and neoadjuvant chemotherapy had shorter DFS. The only variable identified as a prognostic factor for DFS in the multivariate analysis was IF $CD3^{high}$ T-cell infiltrate (HR = 0.31, 95% CI: 0.15-0.67, $P = 0.002$). DFS was significantly better in patients with high IF CD3 expression (IHC 2-3) than in those with low IF CD3 expression (median DFS of 2.2 years, 95% CI: 1.2-3.9 versus 0.59 years, 95% CI: 0.13-1.13, respectively, HR = 0.36, $P = 0.005$, **Fig. 2A**).

A similar pattern of differential DFS according to the IF $CD3^{high}$ score in metastases was observed when the analysis was restricted to patients with synchronous metastases (**Fig. S4**). Given the relatively small size of our cohort, we did not analyze IF $CD3^{high}$ T cell expression impact on DFS in patients with metachronous metastases.

According to stratification based on PD-L1 expression by immune cells in metastases, the median DFS was significantly better in patients with high PD-L1 expression (the median DFS = 2.56 years, 95% CI: 1.11-8.34 versus 1.17 years, 95% CI: 0.73-2.22, respectively, HR = 0.58, 95% CI: 0.34-1.02, $P = 0.05$, **Fig. 2B**). The DFS was not significantly different regarding metastatic $CD8^{high}$ expression in stroma or at the IF.

A schematic graphical summary of the key points is presented in **Fig. S5**.

4. DISCUSSION

Assessment of tumor-immune infiltrating cells is emerging as an important prognostic tool to stratify cancer patients according to the immune microenvironment. However, there are currently limited data on such analysis between the primary and paired metastatic tumor in patients with mCRC. In this study, we observed the intra-patient heterogeneity of immune infiltrates in both chemotherapy-naive primary tumors and in the matched metastases (mainly in the liver) in 74 patients with mCRC.

Many studies explored immune infiltrate across tumorigenesis, with approaches outlining the difference in the immune contexture between primary and metastatic tumors [38-39]. In the study by Angelora et al., a thorough genomic and immunological characterization of primary and the matched metastatic tumor of two patients with CRC did not show any correlation, suggesting a high level of tumor heterogeneity between all lesions [38]. This observation was further clearly confirmed by a Consensus Molecular Subtype (CMS) characterization in omCRC patients [39]. The authors showed that CMS subtypes, determined in patients undergoing partial hepatectomy of resectable CRC liver metastases, were variable. Gene expression analysis showed the absence of CMS1 (1%) and CMS3 (0%) subtypes in liver metastases and their presence in in the primary tumors (14% and 13%, respectively). Therefore, the immune profiling performed on the primary CRC has a limited predictive value to estimate the immune contexture in metastases.

In our analysis, the immune infiltrate in the primary tumor was not associated with survival (data not shown), except for stromal FOXP3. Previously published reports showed discordant results regarding the prognostic value of FOXP3 probably reflecting the plasticity of these immune subsets. Our results provide evidence that CD3 score in the IF of metastases has an independent prognostic value for DFS, doubling the survival rate, independent of TRG, further confirming the previously published data [1,13,40]. Contrary to Mlecnik et al. [2], we did not observe higher IF CD3 in patients with lower TRG (data not published). The median DFS was also significantly better in patients with higher immune PD-L1 expression in metastases in our study. In another study, PD-L1 expression in tissue microarray of surgically excised pMMR CRC patients was associated with improved overall survival, but analyses were performed only on primary tumors [20]. Considering these observations, it appears more pertinent to explore and characterize the immune infiltrate of metastases and to correlate it with patient prognosis for stratification of patients for appropriate therapies.

An efficient immune response is characterized by activation of the interferon signaling pathway generating mature cytotoxic lymphocytes. PD-L1 expression on tumor or immune cells is induced by an interferon-mediated signaling and hence a subpopulation of patients with such expression seems to be of particular interest. In general, $CD8^{high}$/PD-L1 ^{high} cells were previously described as functional effector cells as they produce significantly higher level of Interferon Gamma (IFN-γ) and express more the degranulation marker CD107a than $CD8^{low}$/$PD\text{-}L1^{low}$ cells [41]. Although we did not assessed survival for the immune PD-L1 and $CD8^{high}$ groups due to the small number of patients in each group, the characterization of this subgroup was of importance in pMMR CRC patients. For the first time, we showed that this entity seems to be associated with lower tumoral mass and lower CEA. Lower stroma stiffness is one of the hypotheses explaining the enhancement of the $CD8^{high}$/$PD\text{-}L1^{high}$ population, supported by recent observation correlating desmoplastic angiogenic stroma and $CD8^{high}$ T cell immune infiltration in CRC liver metastasis [42]. This is in accordance with the previous observations by Wang et al. [40], showing the immune infiltrate associated with metastatic size, number of metastases, and Fong clinical Risk Score in resected CRC liver metastases.

The effect of chemotherapy on the $CD8^{high}$/$PD\text{-}L1^{high}$ signature is of importance to better personalize treatment strategies. In our cohort, we observed significantly more patients harboring $CD8^{high}$/$PD\text{-}L1^{high}$ staining in the group exposed to neoadjuvant FOLFOX-based chemotherapy. The T lymphocyte density and location in metastatic melanomas were reported to have predictive value for treatment outcome of patients receiving anti-PD-1/PD-L1 therapies [43]. Although an increase in $CD8^{high}$ and PD-L1 immune infiltrate by chemotherapy did not significantly correlate with survival, we hypothesize that this specific subgroup of patients as identified herein may benefit from personalized treatment including immune checkpoint inhibitors. Effect of chemotherapy on the immune infiltrate was described in non-metastatic rectal cancer, with an increased stromal $CD8^{high}$ and CD4 T cells after chemoradiotherapy, associated with a better prognosis [44]. Recently, the pooled analysis of post-chemotherapy resected metastases of pMMR CRC confirmed the good prognosis of patients with such an inflamed microenvironment [23]. However, this analysis did not include paired tumors before and after treatment. Using a combination of chemotherapies with immune checkpoint inhibitors may improve response rate, as recent data showed up to 27% of pathological response in pMMR CRC patients after nivolumab and ipilimumab neoadjuvant therapy [19]. The tissue immune profiling could allow design of immunotherapies for the $CD8^{high}$/$PD\text{-}L1^{high}$ subset of patients in the adjuvant setting of

metastasectomy. It could also help to plan strategies in the following chemo-immunotherapy lines of treatment. This is consistent with the recent results reported by Kumagai et al. [45] showing that a profound reactivation of effector PD-$1^{+}CD8^{+}$ T cells is necessary for tumor regression, which paves the way for a promising predictive biomarker for PD-1 blockade therapies.

Our study has several limitations. Firstly, the immune infiltrate was investigated in only one metastatic lesion per patient. A major obstacle to a refined definition of the immune contexture of human CRC liver metastases resides in the heterogeneity between the different metastases in the same patient, in addition to the profound heterogeneity of tumor lesions across patients. Galon et al. demonstrated that the immune phenotype of the least-infiltrated metastasis had a stronger association with patient outcome than other metastases [6]. This effort of selection could not be performed here. Nevertheless, in our study, IHC analyses were performed with the semi-quantitative method on the entire slide within three separate compartments of the tumor. Secondly, this study does not include *RAS* mutational status. It was reported that CRC harboring *RAS* mutations or Mitogen-activated protein kinase kinase (MEK) activation had less major histocompatibility complex-I (MHC-I) expression and lower CD8 T cell activation [46]. Neoadjuvant chemotherapy was previously shown to enhance CD8 and immune PD-L1 expression in metastases of *RAS* wild-type cancers [47], and this will be crucial to analyze in validation cohorts. Finally, the peripheral immune response could not be assessed in complement to the intra-tumoral approach. The initiation of cell death and subsequent activation of T cells when antigens are released can be monitored by different methods. The peripheral immune response against tumor antigens before and after administration of the FOLFOX regimen has been previously assessed in mCRC patients [48]. An epitope spreading stimulating immune response against a broad spectrum of tumor antigens hinders monitoring the effect of immune-based chemotherapy in the circulating blood of patients. Peripheral blood leucocytes phenotypic profiling is easy to perform and decreased levels of myeloid-derived suppressor cells (MDSC) and increased levels of circulating CD8+ T cells lymphocytes after 5-fluorouracil-based chemotherapy have been detected by flow cytometric analyzes [49]. Doublet chemotherapies with the FOLFOX +/- bevacizumab induce a significant decrease in the number of MDSC, specifically granulocytic MDSC, which was associated with better progression-free survival in patients receiving this combination [50-51]. A combined peripheral and intra-tumoral assessment of the immune response is a promising approach for the future studies.

5. CONCLUSION

In conclusion, our findings suggest an effect of chemotherapy on modifying the immune microenvironment in resected CRC metastases and highlight the relevance of $CD8^{high}$/$PD\text{-}L1^{high}$ in pMMR/MSS metastases for adjuvant treatments including immunotherapy strategies. This key immune signature based on the assessment of CD8 and PD-L1 by IHC, adapted for a routine practice and a cost-effective method, paves the way for further prospective analyses in mCRC and encourages the efforts for such rare data sharing.

ACKNOWLEDGMENTS

We thank Linh Pham for managing the project. The authors also thank the technical staff of the Department of Pathology of Pitié-Salpêtrière and Magdalena Benetkiewicz (Sc.D.; GERCOR) for editorial assistance.

Data Accessibility:

The datasets used and/or analyzed during the present study are available within the supplementary figures and tables.

Disclosure: The authors have declared no conflict of interest.

Author contributions

MJ: Formal analysis, Validation, Writing-original draft

WWL: Statistical analysis, Critically reviewal of the manuscript

DY: Formal analysis, Critically reviewal of the manuscript

IB Statistical analysis, Critically reviewal of the manuscript

AM, EC, AT, RC, DV: Critically reviewal of the manuscript

IB: Data curation, Critically reviewal of the manuscript

NR, PB, FPL: Complementary investigation, Critically reviewal of the manuscript

TA: Conceptualization, Formal analysis, Validation, Investigation, Critically reviewal of the manuscript

CB, KS: Formal analysis, Validation, Critically reviewal of the manuscript

MS: Conceptualization, Data curation, Formal analysis, Validation, Investigation, Writing-original draft

Financial support: No funding was received for this article.

REFERENCES

1. Galon J, Costes A, Sanchez-Cabo F, Kirilovsky A, Mlecnik B, Lagorce-Pagès C, Tosolini M, Camus M, Berger A, Wind P, et al (2006). Type, density, and location of immune cells within human colorectal tumors predict clinical outcome. Science 313,1960–4.
2. Mlecnik B, Tosolini M, Kirilovsky A, Berger A, Bindea G, Meatchi T, Bruneval P, Trajanoski Z, Fridman WH, Pagès F, et al (2011). Histopathologic-Based Prognostic Factors of Colorectal Cancers Are Associated With the State of the Local Immune Reaction. J Clin Oncol. American Society of Clinical Oncology 29,610–8.
3. Siegel RL, Miller KD, Sauer AG, Fedewa SA, Butterly LF, Anderson JC, Cercek A, Smith RA, Jemal A (2020). Colorectal cancer statistics. CA Cancer J Clin. 70,145–64.
4. Manfredi S, Lepage C, Hatem C, Coatmeur O, Faivre J, Bouvier A-M (2006). Epidemiology and management of liver metastases from colorectal cancer. Ann Surg. 244, 254–9.
5. Rubbia-Brandt L, Giostra E, Brezault C, Roth AD, Andres A, Audard V, Sartoretti P, Dousset B, Majno PE, Soubrane O, et al (2007). Importance of histological tumor response assessment in predicting the outcome in patients with colorectal liver metastases treated with neo-adjuvant chemotherapy followed by liver surgery. Ann Oncol Off J Eur Soc Med Oncol. 18, 299–304.
6. Van den Eynde M, Mlecnik B, Bindea G, Fredriksen T, Church SE, Lafontaine L, Haicheur N, Marliot F, Angelova M, Vasaturo A, et al (2018). The Link between the Multiverse of Immune Microenvironments in Metastases and the Survival of Colorectal Cancer Patients. Cancer Cell 34, 1012-1026.e3.
7. Halama N, Michel S, Kloor M, Zoernig I, Benner A, Spille A, Pommerencke T, von Knebel DM, Folprecht G, Luber B, et al (2011). Localization and density of immune cells in the invasive margin of human colorectal cancer liver metastases are prognostic for response to chemotherapy. Cancer Res. 71, 5670–7.
8. Maker AV, Ito H, Mo Q, Weisenberg E, Qin L-X, Turcotte S, Maithel S, Shia J, Blumgart L, Fong Y, et al (2015). Genetic evidence that intratumoral T-cell proliferation and activation are associated with recurrence and survival in patients with resected colorectal liver metastases. Cancer Immunol Res. 3, 380–8.
9. Halama N, Spille A, Lerchl T, Brand K, Herpel E, Welte S, Keim S, Lahrmann B, Klupp F, Kahlert C, et al (2013). Hepatic metastases of colorectal cancer are rather homogeneous but

differ from primary lesions in terms of immune cell infiltration. Oncoimmunology. 2:e24116.
10. Zwing N, Failmezger H, Ooi C-H, Hibar DP, Cañamero M, Gomes B, Gaire F, Korski K (2020). Analysis of Spatial Organization of Suppressive Myeloid Cells and Effector T Cells in Colorectal Cancer—A Potential Tool for Discovering Prognostic Biomarkers in Clinical Research. Front Immunol. 11, 550250
11. Zitvogel L, Apetoh L, Ghiringhelli F, André F, Tesniere A, Kroemer G (2008). The anticancer immune response: indispensable for therapeutic success? J Clin Invest. 118, 1991–2001.
12. Vanmeerbeek I, Sprooten J, De Ruysscher D, Tejpar S, Vandenberghe P, Fucikova J, Spisek R, Zitvogel L, Kroemer G, Galluzzi L, et al (2020). Trial watch: chemotherapy-induced immunogenic cell death in immuno-oncology. Oncoimmunology 9, 1703449.
13. Tanis E, Julié C, Emile J-F, Mauer M, Nordlinger B, Aust D, Roth A, Lutz MP, Gruenberger T, Wrba F, et al (2015). Prognostic impact of immune response in resectable colorectal liver metastases treated by surgery alone or surgery with perioperative FOLFOX in the randomised EORTC study 40983. Eur J Cancer 51, 2708–17.
14. Le DT, Uram JN, Wang H, Bartlett BR, Kemberling H, Eyring AD, Skora AD, Luber BS, Azad NS, Laheru D, et al (2015). PD-1 Blockade in Tumors with Mismatch-Repair Deficiency. N Engl J Med. 372, 2509–20.
15. Le DT, Durham JN, Smith KN, Wang H, Bartlett BR, Aulakh LK, Lu S, Kemberling H, Wilt C, Luber BS, et al (2017). Mismatch-repair deficiency predicts response of solid tumors to PD-1 blockade. Science 357, 409–13.
16. Overman MJ, McDermott R, Leach JL, Lonardi S, Lenz H-J, Morse MA, Desai J, Hill A, Axelson M, Moss RA, et al (2017). Nivolumab in patients with metastatic DNA mismatch repair-deficient or microsatellite instability-high colorectal cancer (CheckMate 142): an open-label, multicentre, phase 2 study. Lancet Oncol. 18, 1182–91.
17. Overman MJ, Lonardi S, Wong KYM, Lenz H-J, Gelsomino F, Aglietta M, Morse MA, Van Cutsem E, McDermott R, Hill A, et al (2018). Durable Clinical Benefit With Nivolumab Plus Ipilimumab in DNA Mismatch Repair-Deficient/Microsatellite Instability-High Metastatic Colorectal Cancer. J Clin Oncol Off J Am Soc Clin Oncol. 36, 773–9.
18. André T, Shiu K-K, Kim TW, Jensen BV, Jensen LH, Punt C, Smith D, Garcia-Carbonero R, Benavides M, Gibbs P, et al (2020). Pembrolizumab in Microsatellite-Instability-High Advanced Colorectal Cancer. N Engl J Med. 383, 2207–18.

19. Chalabi M, Fanchi LF, Dijkstra KK, Van den Berg JG, Aalbers AG, Sikorska K, Lopez-Yurda M, Grootscholten C, Beets GL, Snaebjornsson P, et al (2020). Neoadjuvant immunotherapy leads to pathological responses in MMR-proficient and MMR-deficient early-stage colon cancers. Nat Med. 26, 566–76.
20. Droeser RA, Hirt C, Viehl CT, Frey DM, Nebiker C, Huber X, Zlobec I, Eppenberger-Castori S, Tzankov A, Rosso R, et al (2013). Clinical impact of programmed cell death ligand 1 expression in colorectal cancer. Eur J Cancer 49, 2233–42.
21. Li Y, Liang L, Dai W, Cai G, Xu Y, Li X, Li Q, Cai S (2016). Prognostic impact of programed cell death-1 (PD-1) and PD-ligand 1 (PD-L1) expression in cancer cells and tumor infiltrating lymphocytes in colorectal cancer. Mol Cancer 15:55.
22. Masugi Y, Nishihara R, Yang J, Mima K, da Silva A, Shi Y, Inamura K, Cao Y, Song M, Nowak JA, et al (2017). Tumour CD274 (PD-L1) expression and T cells in colorectal cancer. Gut. 66, 1463–73.
23. Moretto R, Corallo S, Belfiore A, Rossini D, Boccaccino A, Lonardi S, Centonze G, Morano F, Germani MM, Loupakis F, et al (2020). Prognostic impact of immune-microenvironment in colorectal liver metastases resected after triplets plus a biologic agent: A pooled analysis of five prospective trials. Eur J Cancer Oxf Engl 1990. 135, 78–88.
24. Berntsson J, Eberhard J, Nodin B, Leandersson K, Larsson AH, Jirström K (2018). Expression of programmed cell death protein 1 (PD-1) and its ligand PD-L1 in colorectal cancer: Relationship with sidedness and prognosis. Oncoimmunology 7:e1465165.
25. Ni X, Sun X, Wang D, Chen Y, Zhang Y, Li W, Wang L, Suo J (2019). The clinicopathological and prognostic value of programmed death-ligand 1 in colorectal cancer: a meta-analysis. Clin Transl Oncol. 21(5), 674-686.
26. Ahtiainen M, Elomaa H, Väyrynen JP, Wirta EV, Kuopio T, Helminen O, Seppälä TT, Kellokumpu I, Mecklin JP (2021). Immune Contexture of MMR-Proficient Primary Colorectal Cancer and Matched Liver and Lung Metastases. Cancers (Basel) 13(7), 1530.
27. Hebbar M, Chibaudel B, André T, Mineur L, Smith D, Louvet C, Dutel JL, Ychou M, Legoux JL, Mabro M, et al (2015). FOLFOX4 versus sequential dose-dense FOLFOX7 followed by FOLFIRI in patients with resectable metastatic colorectal cancer (MIROX): a pragmatic approach to chemotherapy timing with perioperative or postoperative chemotherapy from an open-label, randomized phase III trial. Ann Oncol. 26, 340–7.
28. Dahlin AM, Henriksson ML, Van Guelpen B, Stenling R, Oberg A, Rutegård J, Palmqvist R

(2011). Colorectal cancer prognosis depends on T-cell infiltration and molecular characteristics of the tumor. Mod Pathol Off J U S Can Acad Pathol Inc. 24, 671–82.

29. Ma C, Patel K, Singhi AD, Ren B, Zhu B, Shaikh F, Sun W (2016). Programmed Death-Ligand 1 Expression Is Common in Gastric Cancer Associated With Epstein-Barr Virus or Microsatellite Instability. Am J Surg Pathol. 40, 1496–506.

30. Hellmann MD, Kim T-W, Lee CB, Goh B-C, Miller WH, Oh D-Y, et al (2019). Phase Ib study of atezolizumab combined with cobimetinib in patients with solid tumors. Ann Oncol Off J Eur Soc Med Oncol. 30, 1134–42

31. Kong P, Wang J, Song Z, Liu S, He W, Jiang C, et al (2019). Circulating Lymphocytes, PD-L1 Expression on Tumor-infiltrating Lymphocytes, and Survival of Colorectal Cancer Patients with Different Mismatch Repair Gene Status. J Cancer 10, 1745–54.

32. Taube JM, Klein A, Brahmer JR, Xu H, Pan X, Kim JH, et al (2014). Association of PD-1, PD-1 ligands, and other features of the tumor immune microenvironment with response to anti-PD-1 therapy. Clin Cancer Res Off J Am Assoc Cancer Res. 20, 5064–74.

33. Kim JH, Park HE, Cho N-Y, Lee HS, Kang GH (2016). Characterisation of PD-L1-positive subsets of microsatellite-unstable colorectal cancers. Br J Cancer 115, 490–6.

34. Lee KS, Kim BH, Oh H-K, Kim D-W, Kang S-B, Kim H, et al (2018). Programmed cell death ligand-1 protein expression and CD274/PD-L1 gene amplification in colorectal cancer: Implications for prognosis. Cancer Sci. 109, 2957–69.

35. Chen DS, Mellman I (2017). Elements of cancer immunity and the cancer-immune set point. Nature 541, 321–30.

36. Müller P, Kreuzaler M, Khan T, Thommen DS, Martin K, Glatz K, Savic S, Harbeck N, Nitz U, Gluz O, et al (2015). Trastuzumab emtansine (T-DM1) renders HER2+ breast cancer highly susceptible to CTLA-4/PD-1 blockade. Sci Transl Med. 7, 315ra188.

37. Yamaguchi T, Teraguchi S, Furusawa C, Machiyama H, Watanabe TM, Fujita H, Sakaguchi S, Yanagida T (2019). Theoretical modeling reveals that regulatory T cells increase T-cell interaction with antigen-presenting cells for stable immune tolerance. Int Immunol. 31, 743–53.

38. Angelova M, Mlecnik B, Vasaturo A, Bindea G, Fredriksen T, Lafontaine L, Buttard B, Morgand E, Bruni D, Jouret-Mourin A, et al (2018). Evolution of Metastases in Space and Time under Immune Selection. Cell. 175, 751-765.e16.

39. Pitroda SP, Khodarev NN, Huang L, Uppal A, Wightman SC, Ganai S, Joseph N, Pitt J,

Brown M, Forde M, et al (2018). Integrated molecular subtyping defines a curable oligometastatic state in colorectal liver metastasis. Nat Commun. 9, 1793.

40. Wang Y, Lin H, Huang M, Shao Q, Wang Z, Wang F, Yuan Y, Li B, Wang D, Ding P, et al (2018). The Immunoscore system predicts prognosis after liver metastasectomy in colorectal cancer liver metastases. Cancer Immunol Immunother. 67, 435–44.
41. Liu X, Wu X, Cao S, Harrington SM, Yin P, Mansfield AS, Dong H (2016). B7-H1 antibodies lose antitumor activity due to activation of p38 MAPK that leads to apoptosis of tumor-reactive CD8+ T cells. Sci Rep., 6:36722.
42. Höppener DJ, Nierop PMH, Hof J, Sideras K, Zhou G, Visser L, Gouw ASH, de Jong KP, Sprengers D, Kwekkeboom J, et al (2020). Enrichment of the tumour immune microenvironment in patients with desmoplastic colorectal liver metastasis. Br J Cancer. 123, 196–206.
43. Tumeh PC, Harview CL, Yearley JH, Shintaku IP, Taylor EJM, Robert L, Chmielowski B, Spasic M, Henry G, Ciobanu V, et al (2014). PD-1 blockade induces responses by inhibiting adaptive immune resistance. Nature 515, 568–71.
44. Teng F, Mu D, Meng X, Kong L, Zhu H, Liu S, Zhang J, Yu J (2015). Tumor infiltrating lymphocytes (TILs) before and after neoadjuvant chemoradiotherapy and its clinical utility for rectal cancer. Am J Cancer Res. 5, 2064–74.
45. Kumagai S, Togashi Y, Kamada T, Sugiyama E, Nishinakamura H, Takeuchi Y, Vitaly K, Itahashi K, Maeda Y, Matsui S, et al (2020). The PD-1 expression balance between effector and regulatory T cells predicts the clinical efficacy of PD-1 blockade therapies. Nat Immunol. 21, 1346–58.
46. Ebert PJR, Cheung J, Yang Y, McNamara E, Hong R, Moskalenko M, Gould SE, Maecker H, Irving BA, Kim JM, et al (2016). MAP Kinase Inhibition Promotes T Cell and Anti-tumor Activity in Combination with PD-L1 Checkpoint Blockade. Immunity 44, 609–21.
47. Ledys F, Klopfenstein Q, Truntzer C, Arnould L, Vincent J, Bengrine L, Remark R, Boidot R, Ladoire S, Ghiringhelli F, et al (2018). RAS status and neoadjuvant chemotherapy impact $CD8^+$ cells and tumor HLA class I expression in liver metastatic colorectal cancer. J Immunother Cancer 6:123.
48. Galaine J, Turco C, Vauchy C, Royer B, Mercier-Letondal P, Queiroz L, Loyon R, Mouget V, Boidot R, Laheurte C, et al (2019). CD4 T cells target colorectal cancer antigens upregulated by oxaliplatin. Int J Cancer 145, 3112–25.

49. Vincent J, Mignot G, Chalmin F, Ladoire S, Bruchard M, Chevriaux A, Martin F, Apetoh L, Rébé C, Ghiringhelli F (2010). 5-Fluorouracil selectively kills tumor-associated myeloid-derived suppressor cells resulting in enhanced T cell-dependent antitumor immunity. Cancer Res. 70, 3052–61.
50. Kanterman J, Sade-Feldman M, Biton M, Ish-Shalom E, Lasry A, Goldshtein A, et al (2014). Adverse immunoregulatory effects of 5FU and CPT11 chemotherapy on myeloid-derived suppressor cells and colorectal cancer outcomes. Cancer Res. 74, 6022–35.
51. Limagne E, Euvrard R, Thibaudin M, Rébé C, Derangère V, Chevriaux A, et al (2016). Accumulation of MDSC and Th17 Cells in Patients with Metastatic Colorectal Cancer Predicts the Efficacy of a FOLFOX-Bevacizumab Drug Treatment Regimen. Cancer Res. 76, 5241–52.

SUPPORTING INFORMATION

Table S1. Raw data
Table S2. The cohort baseline characteristics
Table S3. Patients' and metastatic biomarkers characteristics according to neoadjuvant or adjuvant chemotherapy
Table S4: Spearman correlation between metastatic immune infiltrate and TRG scoring
Figure S1: Flow chart of the study
Figure S2: Heatmaps of biomarkers expression in the primary and metastatic tumor
Figure S3: Representative images of immunohistochemistry co-staining of CD8 and PD-L1.
Figure S4: Kaplan-Meier curve showing the association between CD3 ^{high} in the invasive front and DFS in mCRC patients with synchronous metastases.
Figure S5: Graphical summary of the results

Table 1. Distribution of biomarkers in the primary tumor and metastatic sites

	IHC	CD3 IF	CD3 stroma	CD3 IE	CD8 IF	CD8 stroma	PD-1 IF	PD-1 stroma	Foxp3 IF	Foxp3 stroma		PD-L1 tumoral cells	PD-L1 immune cells
Primary Tumors													
All (*N* = 74)	**IHC 3+**	11 (14.9%)	15 (20.5%)	14 (19.2%)	0	0	NA	NA	NA	NA			
	IHC 2+ and 3+	33 (44.6%)	42 (57.5)	26 (35.6%)	6 (8.5%)	8 (11.3%)	2 (2.7%)	1 (1.4%)	3 (4.1%)	11 (14.9%)	**≥5%**	5 (6.8%)	42 (57.5%)
	IHC 0+ and 1+	41 (55.4%)	31 (42.5%)	47 (64.4%)	65 (91.5%)	63 (88.7%)	71 (97.3%)	73 (98.6%)	71 (95.9%)	63 (85.1%)	**<5%**	68 (93.2%)	31 (42.5%)
Associated with neo-adjuvant metastases	**IHC 3+**	4 (10.0%)	8 (20.0%)	7 (17.5%)	0	0	NA	NA	NA	NA			
(*N* = 40)	**IHC 2+ and 3+**	16 (40.0%)	22 (55.0%)	13 (32.5%)	2 (5.3%)	5 (13.2%)	1 (2.5%)	0	2 (5.0%)	4 (10.0%)	**≥5%**	2 (5.1%)	22 (56.4%)
	IHC 0+ and 1+	24 (60.0%)	18 (45.0%)	27 (67.5%)	36 (94.7%)	33 (86.8%)	39 (97.5%)	40 (100%)	38 (95.0%)	36 (90.0%)	**<5%**	37 (94.9%)	17 (43.6%)
Associated with chemo-naive metastases	**IHC 3+**	7 (20.6%)	7 (21.2%)	7 (21.2%)	0	0	NA	NA	NA	NA			
(*N* = 34)	**IHC 2+ and 3+**	17 (50.0%)	20 (60.6%)	13 (39.4%)	4 (12.1%)	3 (9.1%)	1 (3.0%)	1 (2.9%)	1 (2.9%)	7 (20.6%)	**≥5%**	3 (8.8%)	20 (58.8%)
	IHC 0+ and 1+	17 (50.0%)	13 (39.4%)	20 (60.6%)	29 (87.9%)	30 (90.9%)	32 (97%)	33 (97.1%)	33 (97.1%)	27 (79.4%)	**<5%**	31 (91.2%)	14 (41.2%)
Metastases													
All (*N* = 74)	**IHC 3+**	16 (21.9%)	10 (13.5%)	12 (16.4%)	2 (2.8%)	3 (4.2%)	NA	NA	NA	NA			
	IHC 2+ and 3+	63 (86.3%)	30 (40.5%)	20 (27.4%)	23 (31.9%)	16 (22.2%)	9 (12.7%)	4 (5.6%)	0	4 (5.6%)	**≥5%**	7 (9.7%)	44 (61.1%)
	IHC 0+ and 1+	10 (13.7%)	44 (59.5%)	53 (72.6%)	49 (68.1%)	56 (77.8%)	62 (87.3%)	67 (94.4%)	72 (100%)	68 (94.4%)	**<5%**	65 (90.3%)	28 (38.9%)
Neoadjuvant	**IHC 3+**	11 (28.2%)	7 (17.5%)	5 (12.5%)	1 (2.6%)	2 (5.1%)	NA	NA	NA	NA			
(*N* = 40)	**IHC 2+ and 3+**	32 (82.1%)	19 (47.5%)	8 (20.0%)	16 (41.0%)	10 (25.6%)	6 (15.8%)	3 (7.9%)	0	0	**≥5%**	5 (13.2%)	21 (55.3%)
	IHC 0+ and 1+	7 (17.9%)	21 (52.5%)	32 (80.0%)	23 (59.0%)	29 (74.4%)	32 (84.2%)	35 (92.1%)	39 (100%)	39 (100%)	**<5%**	33 (86.8%)	17 (44.7%)
Chemo-naive	**IHC 3+**	5 (14.7%)	3 (8.8%)	7 (21.2%)	1 (3.0%)	1 (3.0%)	NA	NA	NA	NA			
(*N* = 34)	**IHC 2+ and 3+**	31 (91.2%)	11 (32.4%)	12 (36.4%)	7 (21.2%)	6 (18.2%)	3 (9.1%)	1 (3.0%)	0	4 (12.1%)	**≥5%**	2 (5.9%)	23 (67.6%)
	IHC 0+ and 1+	3 (8.8%)	23 (37.6%)	21 (63.6%)	26 (78.8%)	27 (81.8%)	30 (90.9%)	32 (97.0%)	33 (100%)	29 (87.9%)	**<5%**	32 (94.1%)	11 (32.4%)

Abbreviations: IHC, immunohistochemistry; IF, invasive front

Table 2. Patients' characteristics according to invasive front CD3, invasive front CD8, and immune cell PD-L1 expressions in chemo-naive patients with metastases

Parameter		Invasive front CD3 in metastases			Invasive front CD8 and immune cells PD-L1 in metastases			
		CD3 high	**CD3 low**	***P***	**CD8high PD-L1 high**	**CD8 low PD-L1 high**	**CD8 low PD-L1 low**	***P***
Age (years)	*N*	31	3		7	16	10	
	Median (range)	**61 (45-75)**	**68 (66-74)**	0.089	**64.2 (45-75)**	**59.6 (50-71)**	**64.6 (53-75)**	0.332
Longest diameter of metastases (cm), *N* (%)	*N*	30	3		7	16	9	
	<=5	29 (96.7)	2 (66.7)	0.176	7 (100.0)	16 (100.0)	7 (77.8)	0.115
	>5	1 (3.3)	1 (33.3)		0 (0.0)	0 (0.0)	2 (22.2)	
N-stage, *N* (%)	*N*	30	3		7	16	9	
	N0	17 (56.7)	1 (33.3)	0.579	4 (57.1)	11 (68.8)	3 (33.3)	0.247
	N+	13 (43.3)	2 (66.7)		3 (42.9)	5 (31.3)	6 (66.7)	
Number of metastases, *N* (%)	*N*	30	3		7	16	9	
	Mean (SD)	1.4 (0.77)	3.3 (3.21)	0.153	1.1 (0.38)	1.6 (0.73)	2.1 (2.09)	0.408
	<=1	21 (70.0)	1 (33.3)	0.252	6 (85.7)	9 (56.3)	6 (66.7)	0.439
	>1	9 (30.0)	2 (66.7)		1 (14.3)	7 (43.8)	3 (33.3)	
Preoperative CEA level (ng/mL)	*N*	28	3		7	16	8	
	Mean (SD)	28.0 (64.22)	6.3 (7.33)	0.640	7.5 (5.17)	13.9 (34.10)	66.0 (105.31)	0.052
Timing of metastases, *N* (%)	*N*	31	3		7	16	10	
	Metachronous	11 (35.5)	1 (33.3)	1.000	2 (28.6)	7 (43.8)	3 (30.0)	0.715
	Synchronous	20 (64.5)	2 (66.7)		5 (71.4)	9 (56.3)	7 (70.0)	
Sex, *N* (%)	*N*	31	3		7	16	10	
	Male	18 (58.1)	3 (100.0)	0.270	6 (85.7)	7 (43.8)	8 (80.0)	0.081
	Female	13 (41.9)	0 (0.0)		1 (14.3)	9 (56.3)	2 (20.0)	
Tumor Sidedness, *N* (%)	*N*	30	3		7	16	10	
	Right-Sided	6 (20.0)	1 (33.3)	0.524	1 (14.3)	3 (18.8)	3 (30.0)	0.742
	Left-Sided(with Rectum)	24 (80.0)	2 (66.7)		6 (85.7)	13 (81.3)	7 (70.0)	

Table 3. Univariate and multivariate analyses for disease-free survival

	Parameter	Univariate analysis		Multivariate analysis	
		HR (95% CI)	***P***	**HR (95% CI)**	***P***
Age (years)		1 (0.970-1.029)	0.951		
Preoperative CEA level		1 (1.000-1.002)	0.130		
Chemotherapy	No	1		1	
	Neoadjuvant	1.99 (1.147-3.453)	**0.014**	1.682 (0.918-3.082)	0.093
Longest diameter of metastases (cm)	<=5	1			
	>5	1.29 (0.604-2.749)	0.513		
N-stage	N0	1			
	N+	1.38 (0.789-2.413)	0.259		
Number of metastases	<=1	1		1	
	>1	2.12 (1.214-3.688)	**0.008**	1.816 (0.987-3.344)	0.055
Timing of metastases	Metachronous	1			
	Synchronous	0.93 (0.489-1.778)	0.832		
TRG	2-3	1			
	4-5	1.02 (0.465-2.256)	0.952		
Sex	Male	1			
	Female	1.41 (0.817, 2.451)	0.216		
Tumor Sidedness	Right-Sided	1			
	Left-Sided(with Rectum)	1.71 (0.728, 4.020)	0.218		
CD3+ IF	Low	1		1	
	High	0.36 (0.175-0.755)	**0.007**	0.309 (0.145-0.657)	**0.002**
CD3+ Stroma	Low	1			
	High	1.19 (0.692-2.032)	0.534		
CD3+ IE	Low	1			
	High	0.71 (0.380-1.333)	0.288		
CD8+ IF	Low	1			
	High	1.21 (0.688-2.133)	0.507		
CD8+ Stroma	Low	1			
	High	1.47 (0.776-2.787)	0.237		
PD-L1 TC	Low	1			
	High	0.80 (0.286-2.213)	0.661		
PD-L1 IC	Low	1			
	High	0.58 (0.335-1.020)	0.059		
CD8+ IF and PD-L1 IC	CD8low PD-L1low	1			
	CD8hi PD-L1hi	0.79 (0.405-1.526)	0.477		
	CD8hi PD-L1low	1.21 (0.278-5.215)	0.803		
	CD8low PD-L1hi	0.48 (0.238-0.981)	**0.044**		
FOXP3 IF	Staining 0	1			
	Staining 1	0.66 (0.313-1.412)	0.288		
FOXP3 Stroma	Staining 0	1			
	Staining 1	0.59 (0.263-1.301)	0.188		

	Staining 2	0.57 (0.138-2.356)	0.437	
PD1 IF	Low	1		
	High	0.49 (0.192-1.264)	0.141	
PD1 Stroma	Low	1		
	High	0.57 (0.138-2.351)	0.437	

Abbreviations: TRG, tumor regression grades; IF, invasive front; IE, intra-epithelial; IC, immune cell; CT, tumor cell

Figure Legends

Figure 1: Representative images of immunohistochemistry staining of CD8 and PD-L1. (A) High CD8 expression in the invasive front of the primary tumor, (B) High PD-L1 expression in the invasive front of the primary tumor of the same patient, (C) High CD8 expression on immune cell in the invasive front of the liver metastasis of the same patient; (D) High PD-L1 expression on immune cell in the invasive front of the liver metastasis of the same patient, (E) High CD8 expression in the invasive front of a liver metastasis of a second patient, (F) High PD-L1 expression in the invasive front of a liver metastasis of the same second patient, (G) High CD8 expression in the invasive front of an ovary metastasis of a third patient, (H) High PD-L1 expression in the invasive front of an ovary metastasis of the same third patient, (I) High CD8 expression in the invasive front of a liver metastasis of a fourth patient, (J) High PD-L1 expression in the invasive front of a liver metastasis of the same fourth patient, (K) High CD8 expression in the invasive front of a liver metastasis of a fifth patient, (L) High PD-L1 expression in the invasive front of a liver metastasis of the same fifth patient.

Scale bar for 1A, 1B, 1C, 1D = 200 µm.

Scale bar for 1E to 1L = 100 µm.

Figure 2: Kaplan-Meier curves showing the association between $CD3^{high}$ T cell and PD-L1 markers and DFS in patients with mCRC. (A) High and low CD3 in the invasive front at the metastatic site (B) High and low PD-L1 expression on immune cells at the metastatic site

CI, confidence interval

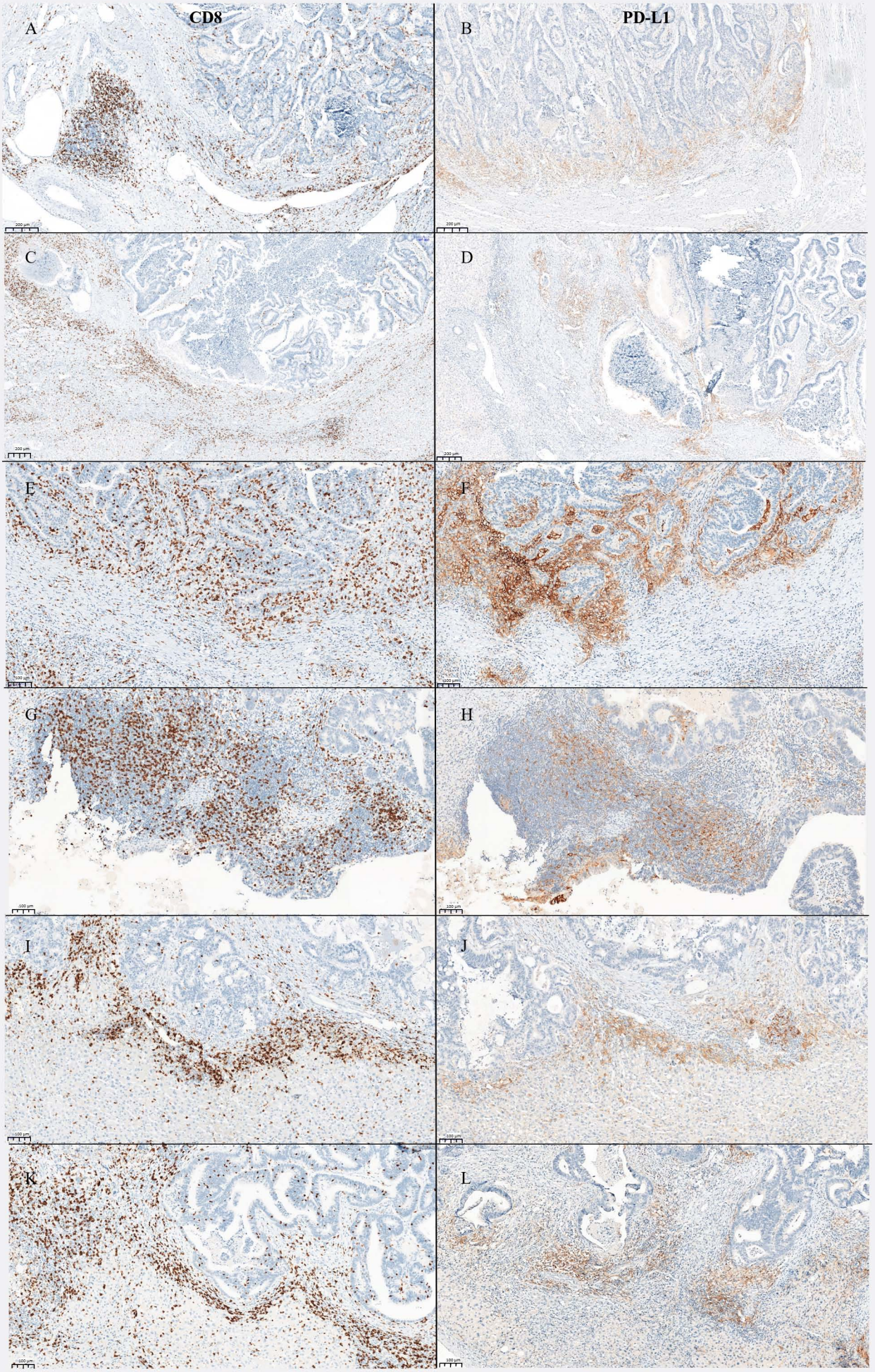
CD8
PD-L1
A
B
C
D
E
F
G
H
I
J
K
L

A

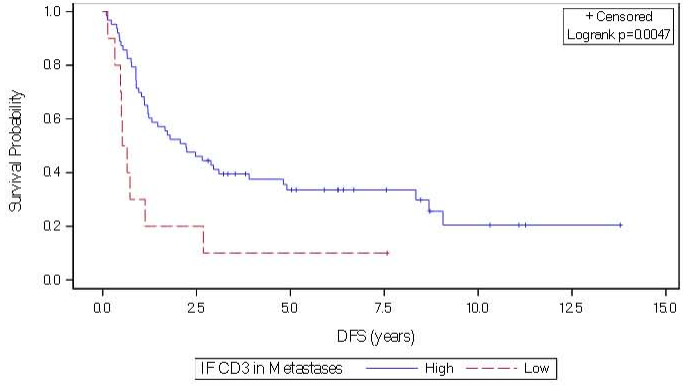

High	63	29	17	10	4	1	0
Low	10	2	1	1	0		

B

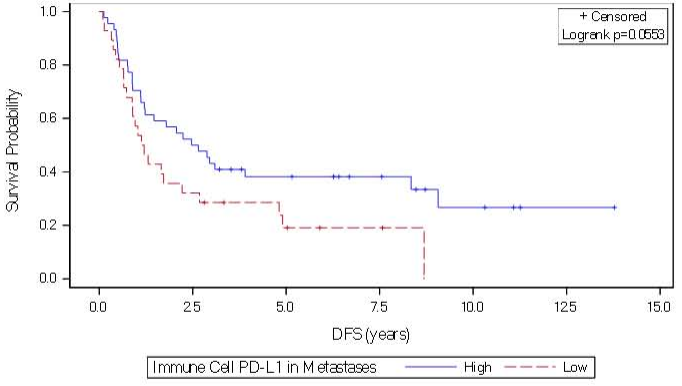

High	44	22	14	9	4	1	0
Low	28	9	4	2	0		